WARSAW UNIVERSITY OF TECHNOLOGY Index 351733
FACULTY OF CIVIL ENGINEERING
COMMITTEE FOR CIVIL AND WATER ENGINEERING
POLISH ACADEMY OF SCIENCES ISSN 1230-2945

DOI: 10.24425/ace.2025.154114

ARCHIVES OF CIVIL ENGINEERING

Vol. LXXI ISSUE 2 2025

pp. 159 –175

Research paper

Experimental investigation on thin-walled steel sigma beams restrained with CFRP textiles

Maciej Adam Dybizbański[1], Katarzyna Rzeszut[2], Hartmut Pasternak[3]

Abstract: Until now, CFRP was used to reinforce steel sections or to extend the service life in the event of fatigue. Now, the aim of the investigations is to find out whether CFRP can be used to convert an open, thin-walled Sigma steel profile into a closed one in certain areas. The tests were carried out on 16 samples, including reference beams (unreinforced) and three different reinforcement solutions as well as two different cross-sections. The experiments included two stages. Both stages used forked supports at each end of the beam, but stage II also blocked the possibility of cross-sectional warping. The laboratory tests used the ARAMIS system and the Artec Leo 3D scanner. The comparative analysis was carried out between vertical and horizontal displacements. In addition, global and local force-displacement diagrams were developed. The proposed reinforcement method can have a significant effect on increasing the load-bearing capacity of thin-walled steel beams with slender cross-sections, which tend to distort in the form of section opening.

Keywords: adhesive connection, CFRP textiles, cold-formed steel, open-closed cross-section, thin-walled beams

[1]MSc., Eng., Poznan University of Technology, Faculty of Civil and Transport Engineering, 5 Marii Skłodowskiej-Curie Str, 60-965 Poznan, Poland, e-mail: maciej.dybizbanski@doctorate.put.poznan.pl, ORCID: 0000-0001-9861-119X
[2]DSc., PhD., Eng., Poznan University of Technology, Faculty of Civil and Transport Engineering, 5 Marii Skłodowskiej-Curie Str, 60-965 Poznan, Poland, e-mail: katarzyna.rzeszut@put.poznan.pl, ORCID: 0000-0002-7134-608X
[3]Prof., DSc., PhD., Eng., Brandenburg University of Technology Cottbus-Senftenberg, Institute of Civil and Structural Engineering, Platz der Deutschen Einheit 1, 03046 Cottbus, Germany, e-mail: hartmut.pasternak@b-tu.de, ORCID: 0000-0003-0473-0302

1. Introduction

Until now, CFRP was used to reinforce steel sections or to extend the service life in the event of fatigue [1–5]. In addition, many problems are posed by the consideration of the existing stress state in the reinforced element, as it usually works in a loaded object [6–9]. It is also extremely problematic to determine the conditions under which the structural strengthening process is carried out, such as access, location and preparation of the surfaces to which the strengthening members are applied, as well as the technological solutions used. It should be emphasized that the method of using CFRP textiles to reinforce structural members is not well recognized in the case of thin-walled cold-formed steel (TWCFS) members [10,11], this method is a new solution and still requires a lot of research and analysis [12–14]. Unfortunately, when such structures are damaged or overloaded, traditional strengthening methods using welded joints or mechanical fasteners are difficult or even impossible to apply. In recent years, the use of CFRP composites as a method of strengthening TWCFS members has become the subject of intensive research by many structural researchers [15–18]. The simplicity and non-destructive nature have made this solution an attractive and effective means of strengthening. CFRP composites are characterized by high strength at very low weight, high corrosion resistance and excellent durability [19]. These characteristics make them particularly useful when the load-bearing capacity needs to be increased and the performance character of TWCFS components needs to be improved. The unquestionable advantage of this method is the non-invasive connection of the reinforcing element to the structure requiring reinforcement, which is particularly useful in the case of TWCFS members.

In this paper the extended investigation [20, 21] of the effects of reinforcing thin-walled cold-formed steel sigma-type beams by sectional closure of their cross-section with glued unidirectional CFRP textiles, also known as CFRP mats, is the main goal of the research.

2. Tests

2.1. Test specimens

TWCFS sigma beams with cross sections of $200 \times 70 \times 2$ and $140 \times 70 \times 2.5$ were tested. The beams were made of S350GD steel. The beams had a 2700 mm span. According to Fig. 1, the CFRP mats were adhered to the edge stiffeners (type 1), the edge stiffeners and flanges (type 2), and the perimeter of the cross-section (type 3).

The formula Eq. (2.1) was used to define and describe the joint length d, which was regarded as the total length of the overlaps of the steel-CFRP bonded joint at each edge of the cross-section:

$$d = \sum_{i=1}^{n} d_i, \tag{2.1}$$

where: n – number of interfaces, d_i – the length of the i-th overlap of the plane of the steel-CFRP bonded joint at the individual edges of the cross-section, shown in Fig. 1.

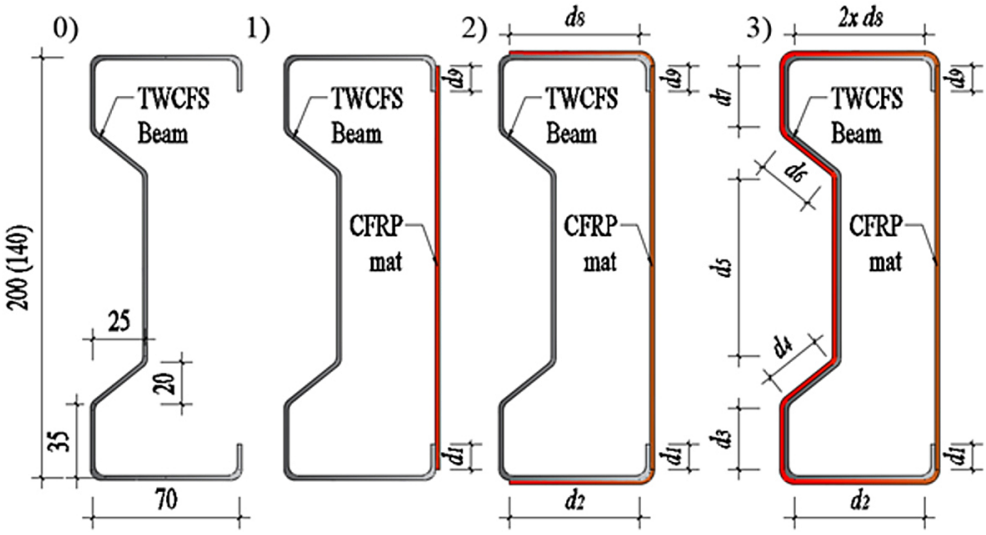

Fig. 1. Geometry of tests beams: 0) reference beam, 1) reinforcement glued on edge stiffeners, 2) reinforcement glued on edge stiffeners and flanges, 3) reinforcement glued around the perimeter of the cross-section

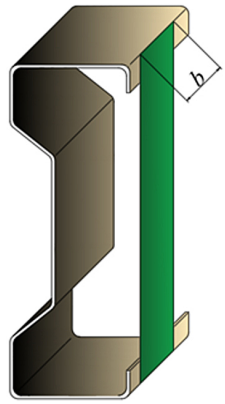

Fig. 2. Reinforcement width *b*

Additionally, a reinforcement width *b* of 300 mm was established (Fig. 2).

A comparison analysis of the displacements obtained for the reinforced beams and the reference (unreinforced) beam served as proof of the reinforcement's influence. Two stages were used in the laboratory tests: stage I considered an ideal fork support and stage II considered a fork support with blocked warping of the cross-section on supports. The aim of the investigations was to find out whether CFRP could be used to convert an open, thin-walled steel profile into a closed one in certain areas.

2.2. Test procedure

The SikaWrap 230 C mat reinforcement was attached to the steel beam with SikaDur 330 adhesive. The beams underwent four-point bending testing. The test bench where supports were intended to serve as fork supports is presented in Fig. 3.

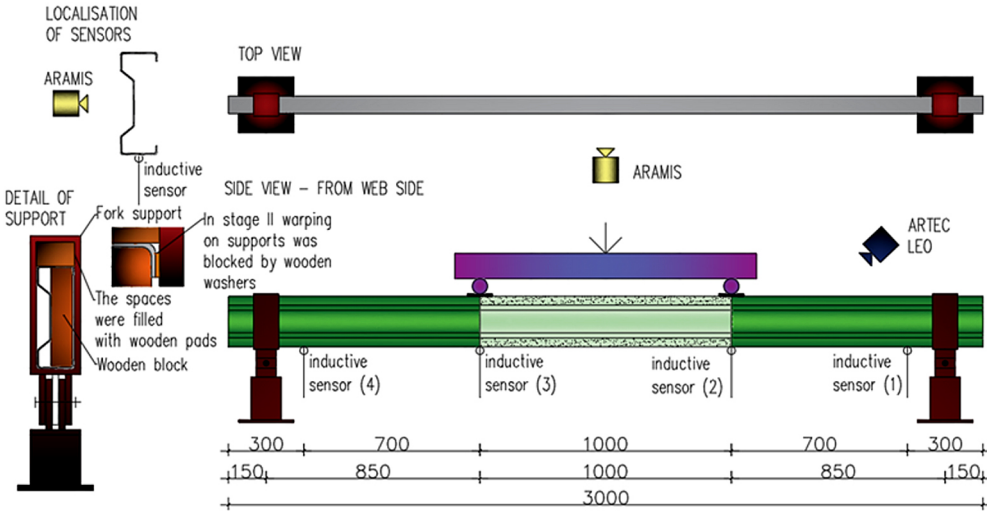

Fig. 3. Scheme of test bench

Additionally, a diaphragm in the form of a wooden block was placed to stiffen the cross section of the beam at the supports. Wooden washers were inserted into any open places between the support and the beam. There were introduced 200 mm and 100 mm wide channel members at the places of force application, respectively for $\sum 200 \times 70 \times 2$ and $\sum 140 \times 70 \times 2.5$ cross-section. The tests were conducted utilizing the INSTRON 8505 testing apparatus, which is capable of applying up to 2400 kN of force. The testing device's piston displacement speed was 1 mm/min. Displacement sensors with measurement ranges of 20 mm and 10 mm were installed at the force application points and 15 cm away from the supports. The deformation data were synchronized with the load increment on the testing machine press and shown as videos and graphs using the ARAMIS 6M optical measurement system. The quantity of photos the system captures throughout the test determines how accurate the results from ARAMIS will be. The equipment was calibrated with a measuring cross prior to each measurement. Throughout the test, image registration was done at a frequency of 2 Hz. Using the GOM Correlate tool, which enables the creation of a spatial model of the beam, the obtained measurements were analyzed. The resultant displacements of beams at particular measurement places were examined in this work. Additionally, a 3D scan of the complete element with 0.1 mm accuracy and a measurement speed of up to 35 million points per second was made using an Artec Leo 3D scanner, which was also utilized to control displacements and inventory the geometry of the beams. When the crosshead was positioned and a force of 0.7 kN was applied, all measuring devices were zeroed.

The geometry of the beam, the force applied to the crosshead, the vertical and horizontal displacements of the beam surface on the web side between the force application positions, and the force applied during positioning, destruction, and after unloading were all measured during the testing.

Each beam was given an individual designation, which consisted of a string of characters, the meaning of which is shown in Table 1.

Table 1. Designations used in naming the samples

Designation	Description
RB	Reference beam
SB	Strengthened beam
H	Section $\sum 200 \times 70 \times 2$
L	Section $\sum 140 \times 70 \times 2.5$
T	Reinforcement width equal to 300 mm
1	Type 1 of reinforcement, according to figure 1
2	Type 2 of reinforcement, according to figure 1
3	Type 3 of reinforcement, according to figure 1
.1	Stage I
.2	Stage II

For example, a beam described as "SBHT1.1" is a reinforced beam of section $\sum 200 \times 70 \times 2$ with a reinforcement width of 300 mm and reinforcement bonded at the edge bends.

2.3. Forms of failure

In none of the cases investigated did the steel-CFRP bonded joint and the CFRP mat fail. In the case of $\sum 200 \times 70 \times 2$ beams, for all specimens, failure occurred through beam lateral-torsional buckling preceded by deformation in the form of section distortion. In addition, local deformation of the top flange occurred at the points of force application. For $\sum 140 \times 70 \times 2.5$ beams, the lateral-torsional buckling did not occur for SBLT1.1 and SBLT2.1 beams. For both stages significant torsion of the cross-section was evident and local deformation of the top flange occurred at the points of force application. A high mutual similarity in the forms of failure of reinforced and unreinforced beams was observed (Figs. 4–7), but it should be emphasized that the reinforcement in the form of CFRP matting allowed a sectional reduction in the opening of the cross-section of the reinforced beams compared to the reference beam.

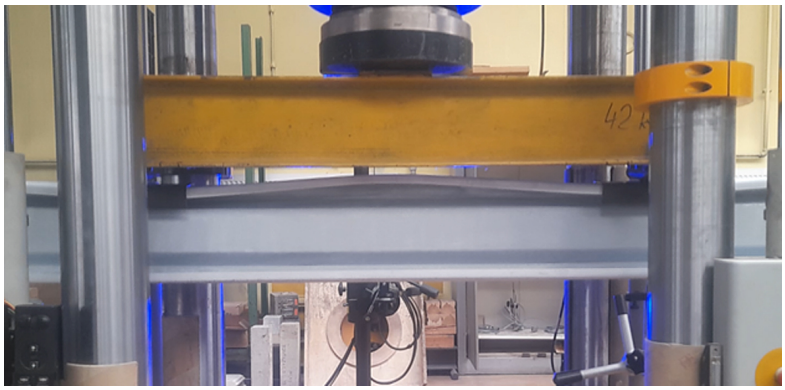

Fig. 4. View of damaged reference beam (unreinforced) Σ 200 × 70 × 2 – RBH.1

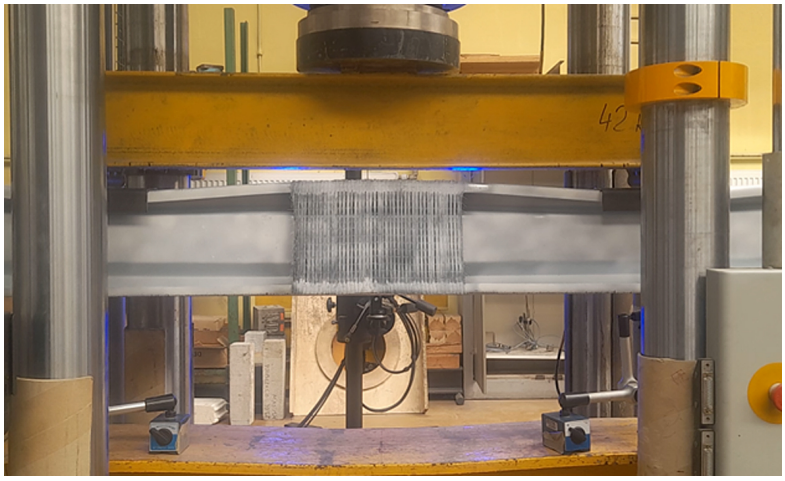

Fig. 5. View of damaged reference beam Σ 200 × 70 × 2 – SBHT1.1

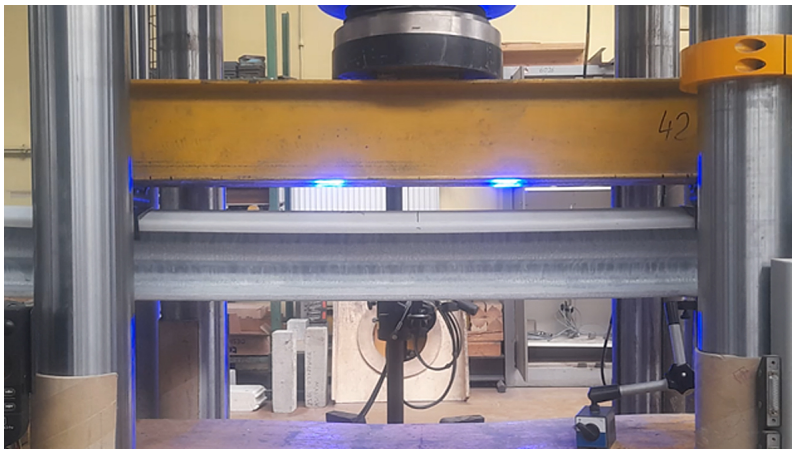

Fig. 6. View of damaged reference beam (unreinforced) Σ 140 × 70 × 2.5 – RBL.1

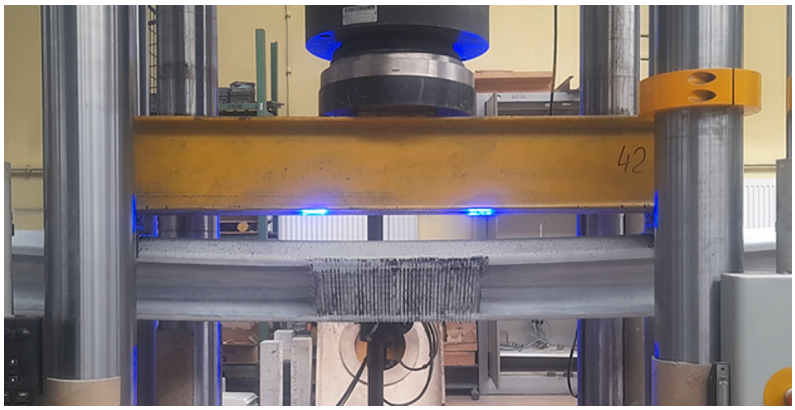

Fig. 7. View of damaged reference beam Σ 140 × 70 × 2.5 – SBLT1.1

2.4. Global force-displacement relations

Figures 8–11 show the global force-displacement relationships for reinforced and reference (unreinforced) beams. The displacement described refers to the vertical displacement of the piston of the testing machine.

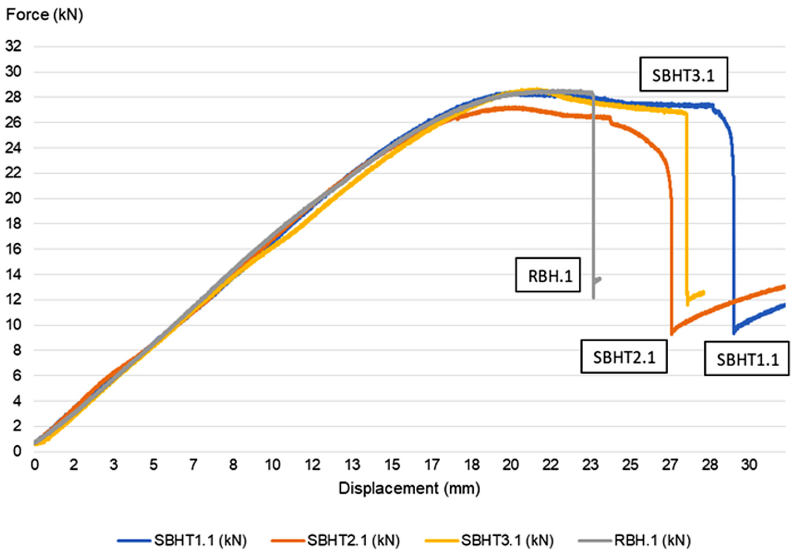

Fig. 8. Global force-displacement relationships for stage I Σ 200 × 70 × 2 beams

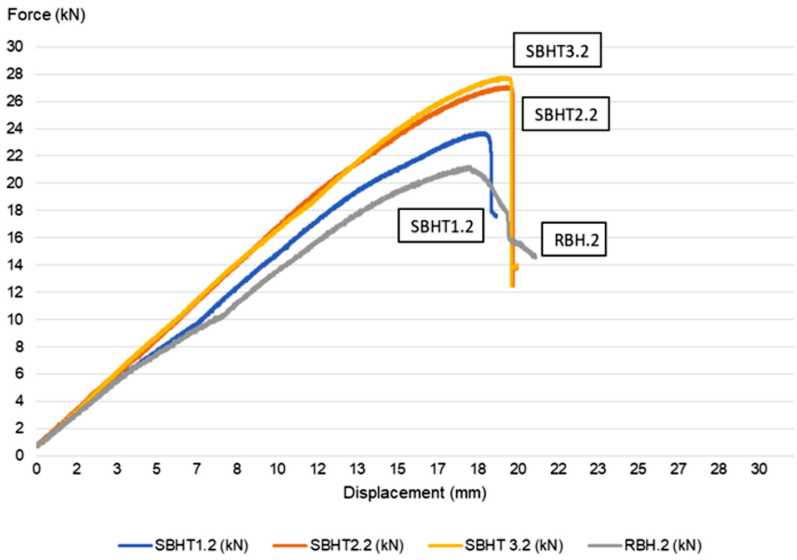

Fig. 9. Global force-displacement relationships for stage II Σ 200 × 70 × 2 beams

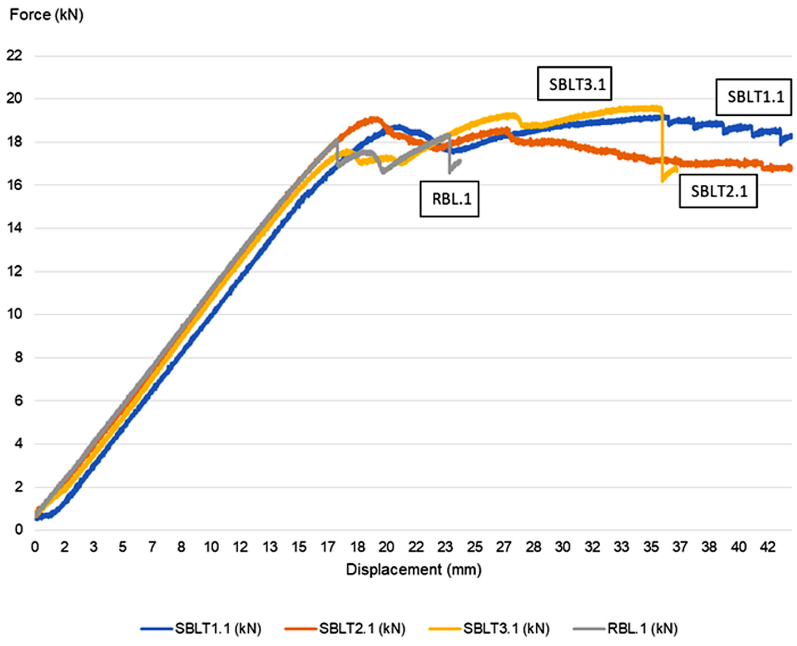

Fig. 10. Global force-displacement relationships for stage I Σ 140 × 70 × 2.5 beams

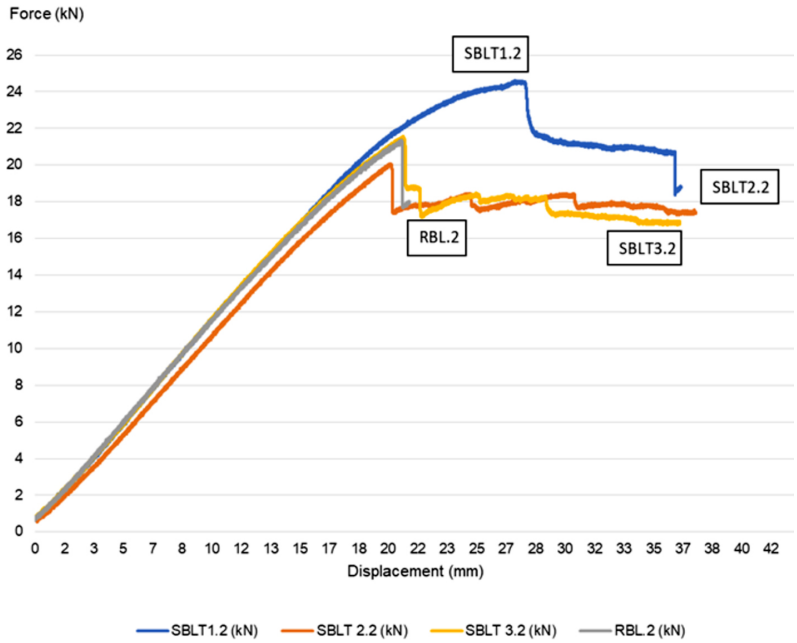

Fig. 11. Global force-displacement relationships for stage II Σ 140 × 70 × 2.5 beams

2.5. Local force-displacement relations

With the usage of ARAMIS system, vertical and horizontal displacement maps were developed for each tested beam. From those maps, the local force-displacement relationships were obtained. Considering ∑ 200 × 70 × 2 beams, four points from vertical displacement maps in planes of applied forces (Y-GL, Y-DL, Y-GP, Y-DP) and three from horizontal displacement maps in the middle of beam span (Z-G, Z-S, Z-D) were chosen (Fig. 12). Similarly, for

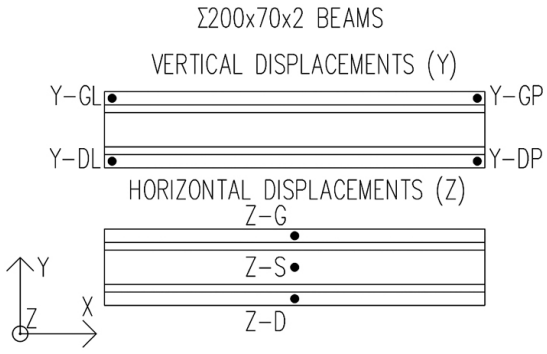

Fig. 12. Localizations of points on web's surface for Σ 200 × 70 × 2 beams

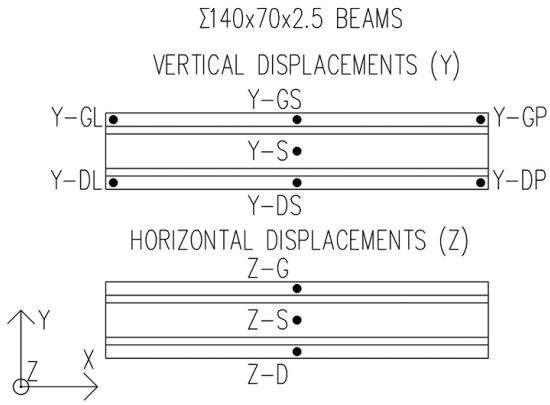

Fig. 13. Localizations of points on web's surface for Σ 140 × 70 × 2.5 beams

$\sum 140 \times 70 \times 2.5$ seven points from vertical displacement maps in planes of applied forces and in the middle of the beam span, as well as, three from horizontal displacement maps in the middle of beam span were chosen (Fig. 13).

Figures 14–17 present chosen local force-displacement relationships for $\sum 200 \times 70 \times 2$ and $\sum 140 \times 70 \times 2.5$ beams, taking into account both vertical and horizontal displacements and both test stages.

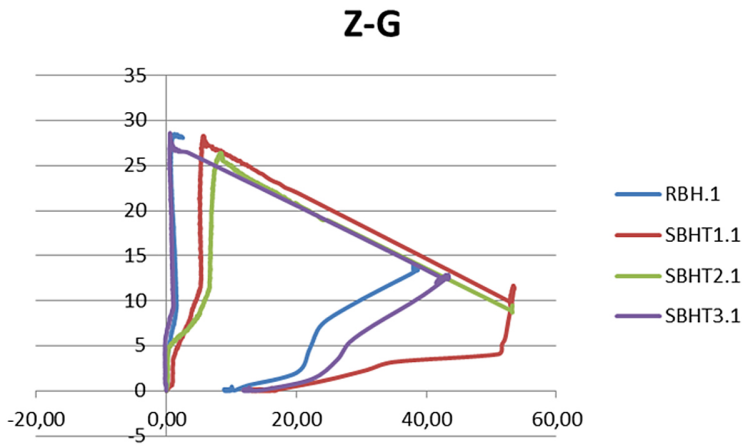

Fig. 14. Local force-dispacement relationship in point Z-G for Σ 200 × 70 × 2 beams in stage I

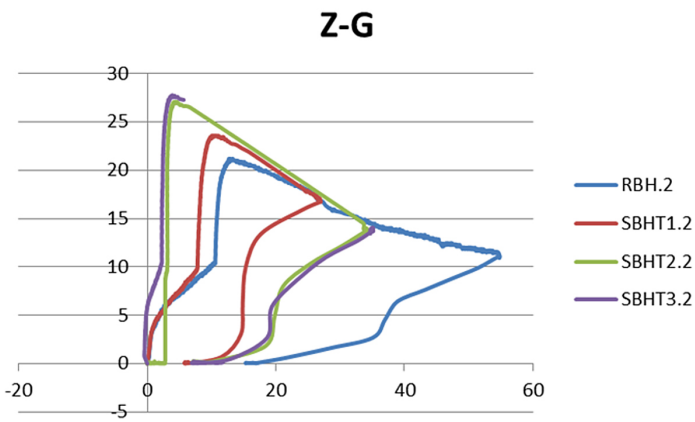

Fig. 15. Local force-dispacement relationship in point Z-G for Σ 200 × 70 × 2 beams in stage II

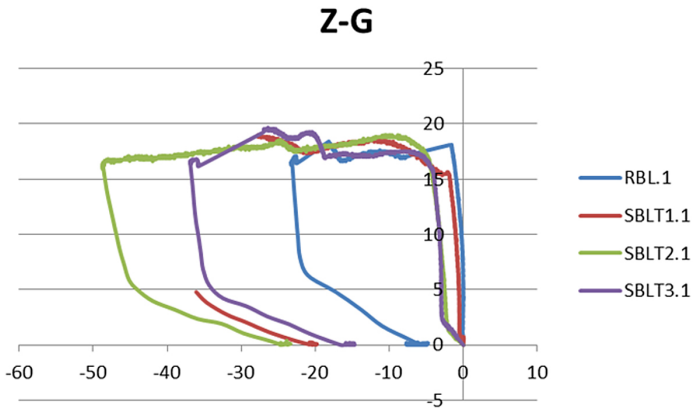

Fig. 16. Local force-dispacement relationship in point Z-G for Σ 140 × 70 × 2.5 beams in stage I

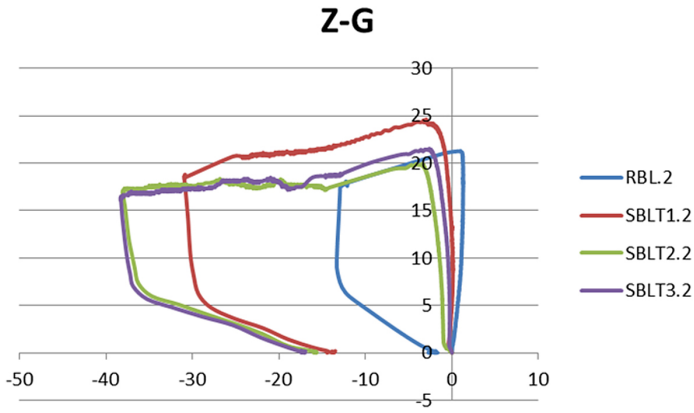

Fig. 17. Local force-dispacement relationship in point Z-G for Σ 140 × 70 × 2.5 beams in stage II

3. Discussion

In order to detect the effect of CFRP mats on thin-walled sigma cold-formed steel beams, a comparative analysis of the values measured during laboratory tests of bare and reinforced beams was carried out. For this purpose, Equations (3.1) and (3.2) ware introduced. The reinforcement influence on the serviceability limit state (LS) was calculated based on Equation (3.1), where LSE^S and LSE^R are the maximum global vertical displacements for strengthened and reference beam respectively; LSS^S and LSS^R are the global vertical displacement for strengthened and reference beam at the beginning of the limit state respectively.

$$LS = \frac{LSE^S - LSS^S}{LSE^R - LSS^R} \cdot 100\% \tag{3.1}$$

Moreover, the reinforcement impact on maximum force (limit point) and displacements coupled with it, the Equation (3.2) was used, where: A is the reinforcement influence on maximum force or displacement, B^S and B^R are maximum force or displacement for strengthened and reinforced beam respectively.

$$A = \frac{B^S}{B^R} \cdot 100\% \tag{3.2}$$

Referring to the above relationships for $\sum 200 \times 70 \times 2$ beams (Fig. 8 for stage I of the study), it can be observed that the global stiffness of the system and the maximum force value achieved are very similar between the reinforced and reference beam. However, the difference is noticeable when the system is operated for a constant force value. The reinforcement allows for extension of limit state for reinforced beams before lateral-torsional buckling by c.a. 17–30% (Fig. 18).

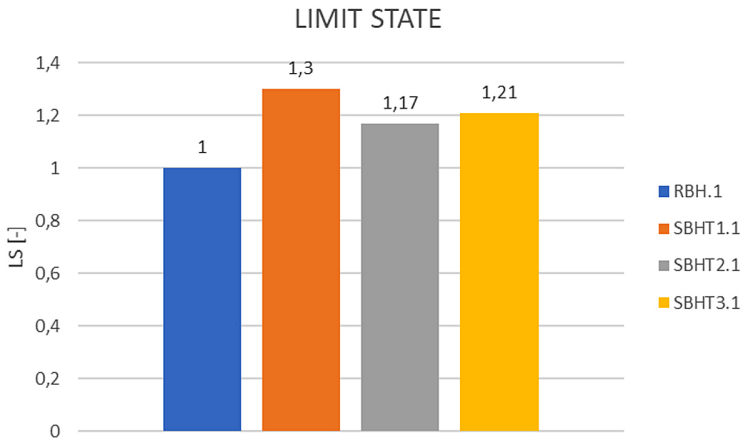

Fig. 18. Reinforcement influence on the limit state for $\sum 200 \times 70 \times 2.0$ beams in stage I

For $\sum 200 \times 70 \times 2$ beams of stage II (Fig. 9), it can be noticed that the global stiffness of the system is very similar between the reinforced and reference beam. All beams collapsed

when the maximum force was reached, with the difference being greater for the reinforced beams. The reinforcement allows an increase in load capacity of 14% for type 1, 28% for type 2 and 33% for type 3 (Fig. 19).

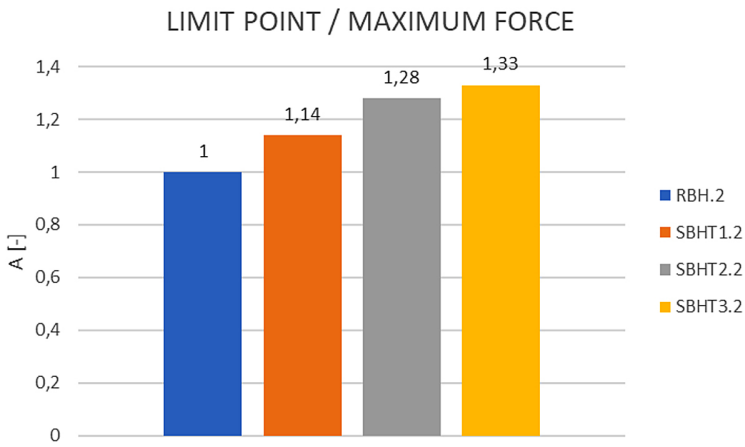

Fig. 19. Reinforcement influence on the limit point for Σ 200 × 70 × 2.0 beams in stage II

Stage I beams of ∑ 140×70×2.5 cross-section (Fig. 10) are characterized by similar stiffness and maximum force value for both reinforced and reference beams. Although, strengthened beams' behavior differs significantly from the reference beam, which failure occurred in form of lateral-torsional buckling. For strengthened beams SBLT1.1 and SBLT2.1 the lateral-torsional buckling did not occur, instead a significant torsion was observed. For SBLT3.1 a significant torsion was noted, followed by lateral-torsional buckling. The reinforcement allows for extension of limit state for reinforced beams before lateral-torsional buckling by at least 50% or may even fully protect against it.

Moreover, for ∑ 140 × 70 × 2.5 beams of stage II the reinforcement have minimal impact on stiffness and maximum load value. The high spike for SBLT1.2 beam may be caused by imperfections of the beam or the laboratory stand.

For ∑ 200 × 70 × 2 beams in stage I, the reinforcement has minimal impact on both vertical and horizontal displacements, however in stage II it may reduce horizontal displacements by c.a. 21–70% (Fig. 20) for top flange and c.a. 24–91% (Fig. 21) in the middle of the web. For ∑ 140 × 70 × 2.5 beams in both stage I and II, the reinforcement has minimal impact on vertical and horizontal displacements. However, it is confirmed that it may extend the limit state of the strengthened beam.

The following observations were formulated on the basis of the analyses carried out:

– In none of the cases investigated did the steel-CFRP bonded joint and the CFRP mat fail.
– In the case of ∑ 200 × 70 × 2 beams, for all specimens, failure occurred through beam lateral-torsional buckling preceded by deformation in the form of cross-section distortion.
– In the case of ∑ 140 × 70 × 2.5 beams, failure occurred through beam lateral-torsional buckling or by large slow torsion of the cross-section.

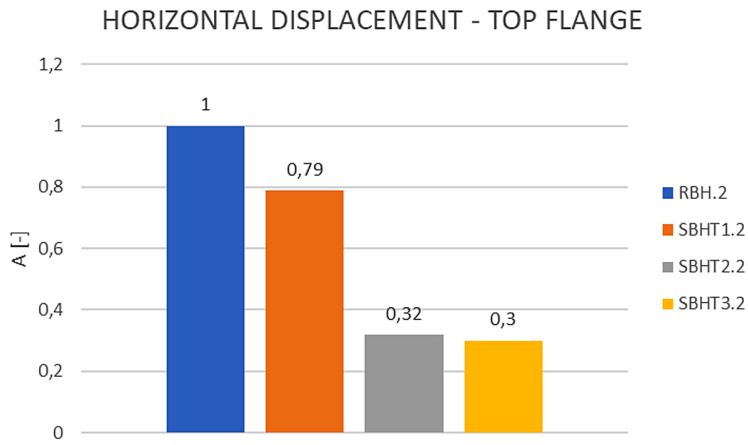

Fig. 20. Reinforcement influence on the top flange horizontal displacement for $\sum 200 \times 70 \times 2.0$ beams in stage II

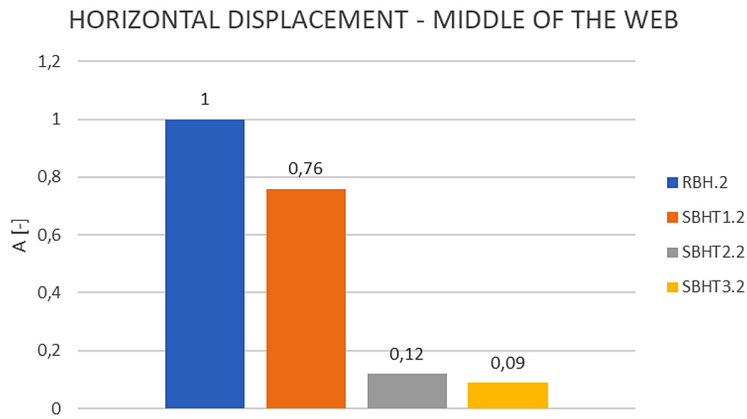

Fig. 21. Reinforcement influence on the top flange horizontal displacement in the middle of the web for $\sum 200 \times 70 \times 2.0$ beams in stage II

- The reinforcement in the form of CFRP matting allowed a sectional reduction in the opening of the cross-section of the reinforced beams compared to the reference beams.
- The reinforcement has minimal impact on global stiffness.
- For $\sum 200 \times 70 \times 2$ beams of stage I the reinforcement allows for longer time of beam's exploitation before its loss of stability by c.a. 17–30% for stage I of $\sum 200 \times 70 \times 2$ beams.
- For $\sum 200 \times 70 \times 2$ beams of stage II the reinforcement allows an increase in load capacity of 14% for type 1, 28% for type 2 and 33% for type 3.
- For $\sum 140 \times 70 \times 2.5$ beams of stage I the reinforcement allows for extension of beam's limit state before lateral-torsional buckling by at least 50% or may even fully protect against it.

– For $\sum 200 \times 70 \times 2$ beams in stage I and $\sum 140 \times 70 \times 2.5$ beams in both stages, the reinforcement has minimal impact on both vertical and horizontal displacements.
– For $\sum 200 \times 70 \times 2$ beams in stage II it may reduce horizontal displacements by c.a. 21–70% for top flange and c.a. 24–91% in the middle of the web.

4. Conclusions

The aim of the investigations was to find out whether CFRP could be used to convert an open, thin-walled steel section into a closed one in certain areas. The aim of this study was to analyse the effect of reinforcing TWCFS sigma beams using pasted unidirectional CFRP fabrics. For this purpose, a series of laboratory tests were carried out on eight beams of type $\sum 200 \times 70 \times 2$ and eight of type $\sum 140 \times 70 \times 2.5$ subjected to four-point bending. The beams were reinforced using SikaWrap 230 C unidirectional CFRP fabric bonded directly to the galvanised layer with SikaDur 330 epoxy-based adhesive such that the fabric was bonded across the cross section in the middle of the beam span to form a closed section. The reinforcement was glued over a width of 300 mm taking into account the three proposed reinforcement methods. Full-scale laboratory tests were carried out using an INSTRON 8505 testing machine, an ARAMIS 6M system and an Artec Leo 3D scanner. Verification of the influence of reinforcement consisted of comparative analysis of vertical and horizontal displacements, as well as maximum force, obtained for reinforced and reference (unreinforced) beams.

The proposed reinforcement method can have a significant effect on increasing the load-bearing capacity of thin-walled steel beams with slender cross-sections, which tend to distort in the form of section opening. In that case the applied fabric prevent the opening of cross-sections and perfectly act against tension. However, one can notice that the CFRP textile, does not work when the cross section is being closed, because in that case the CFRP textile is subjected to compression. Also in the case of stocky cross-sections where the main failure mechanism is lateral-torsional buckling of the beam, the applied reinforcement has a minimal effect on improving the load-bearing capacity of the member. Concluding it must be underline that the applied strengthening method results in a reduction of distorsional deformation in the form of opening of the cross-section resulting from the presence of distorsional moment in accordance with the Jonsson beam theory [22]. In addition, it limits the reduction of geometric characteristics of the cross-section resulting from its opening. In order to improve the load-bearing capacity, it is sufficient to apply the bonded connections of the fabric only at the lip stiffeners. The proposed reinforcement method is easy to apply and has a minimal effect on increasing the weight of the structural member. Such reinforcement has the potential to be applied to existing structures for repair, revitalization or to extend their service life. However, further research is needed to develop precise application guidelines for such a method.

Acknowledgements

The research was financially supported by Poznan University of Technology: 0412/SBAD/0070, 0412/SBAD/0071.

References

[1] S. Bartholomé, et al., "Bonded CFRP lamellae reinforced steel members", A*dhäsion KLEBEN & DICHTEN*, vol. 60, no. 9, pp. 42–49, 2016, doi: 10.1007/s35145-016-0039-6 (in German).

[2] D. Guo, Y.-L. Liu, W.-Y. Gao, and J.-G. Dai, "Bond behavior of CFRP-to-steel bonded joints at different service temperatures: Experimental study and FE modeling", *Construction and Building Materials*, vol. 362, art. no. 129836, 2023, doi: 10.1016/j.conbuildmat.2022.129836.

[3] D. Guo, H.-P. Wang, Y.-L. Liu, W.-Y. Gao, and J.-G. Dai, "Structural behavior of CFRP-strengthened steel beams at different service temperatures: Experimental study and FE modeling", *Engineering Structures*, vol. 293, art. no. 116646, 2023, doi: 10.1016/j.engstruct.2023.116646.

[4] Y. Doroudi, D. Fernando, A. Hosseini, and E. Ghafoori, "Behavior of cracked steel plates strengthened with adhesively bonded CFRP laminates under Fatigue Loading: Experimental and Analytical Study", *Composite Structures*, vol. 266, art. no. 113816, 2021, doi: 10.1016/j.compstruct.2021.113816.

[5] Y. Kasper, et al., "Application of carbon fibre composite materials for the rehabilitation of fatigue damaged steel structures", in *Advances in Engineering Materials, Structures and Systems: Innovations, Mechanics and Applications.* CRC Press, 2019, pp. 2148–2153, doi: 10.1201/9780429426506-370.

[6] A. Kale, P. Zhang, and S. Soghrati, "Effect of pre-existing microstructural damage and residual stresses on the failure response of carbon fiber reinforced polymers", *International Journal of Non-Linear Mechanics*, vol. 147, art. no. 104248, 2022, doi: 10.1016/j.ijnonlinmec.2022.104248.

[7] A. Skiadopoulos, A. de Castro e Sousa, and D. G. Lignos, "Experiments and proposed model for residual stresses in hot-rolled wide flange shapes", *Journal of Constructional Steel Research*, vol. 210, art. no. 108069, 2023, doi: 10.1016/j.jcsr.2023.108069.

[8] S. Lu, et al., "Effect of residual stress in gradient-grained metals: Dislocation dynamics simulations", *International Journal of Mechanical Sciences*, vol. 256, art. no. 108518, 2023, doi: 10.1016/j.ijmecsci.2023.108518.

[9] D. Kollár, I. Völgyi, and A.L. Joó, "Assessment of residual stresses in welded T-joints using contour method", *Thin-Walled Structures*, vol. 190, art. no. 110966, 2023, doi: 10.1016/j.tws.2023.110966.

[10] G.J. Hancock, "Cold-formed steel structures", *Journal of Constructional Steel Research*, vol. 59, no. 4, pp. 473–487, 2003, doi: 10.1016/S0143-974X(02)00103-7.

[11] K. Rzeszut, I. Szewczak, P. Różyło, and M. Guminiak, "Impact of numerical modelling of kinematic and static boundary conditions on stability of cold-formed sigma beam", *Archives of Civil Engineering*, vol. 69, no. 2, pp. 311–323, 2023, doi: 10.24425/ace.2023.145269.

[12] L. Tong, Q. Yu, and X.-L. Zhao, "Experimental study on fatigue behavior of butt-welded thin-walled steel plates strengthened using CFRP sheets", *Thin-Walled Structures*, vol. 147, art. no. 106471, 2020, doi: 10.1016/j.tws.2019.106471.

[13] A. Bastani, S. Das, and S. Kenno, "Rehabilitation of thin walled steel beams using CFRP Fabric", *Thin-Walled Structures*, vol. 143, art. no. 106215, 2019, doi: 10.1016/j.tws.2019.106215.

[14] P.V. Nhut and Y. Matsumoto, "Experimental analytical and theoretical investigations of CFRP strengthened thin-walled steel plates under shear loads", *Thin-Walled Structures*, vol. 155, art. no. 106908, 2020, doi: 10.1016/j.tws.2020.106908.

[15] I. Szewczak, K. Rzeszut, and P. Rozylo, "Structural behaviour of steel cold-formed sigma beams strengthened with bonded steel tapes", *Thin-Walled Structures*, vol. 159, art. no. 107295, 2021, doi: 10.1016/j.tws.2020.107295.

[16] L. Hu, X. Liang, P. Feng, and H.-T. Li, "Temperature effect on buckling behavior of prestressed CFRP-reinforced steel columns", *Thin-Walled Structures*, vol. 188, art. no. 110879, 2023, doi: 10.1016/j.tws.2023.110879.

[17] M.R. Bambach, H.H. Jama, and M. Elchalakani, "Axial capacity and design of thin-walled steel SHS strengthened with CFRP", *Thin-Walled Structures*, vol. 47, no. 10, pp. 1112–1121, 2009, doi: 10.1016/j.tws.2008.10.006.

[18] L. Hu, P. Feng, W. Gao, and Y. Wang, "Flexural behavior of light steel purlins reinforced by prestressed CFRP laminates", *Thin-Walled Structures*, vol. 174, art. no. 109125, 2022, doi: 10.1016/j.tws.2022.109125.

[19] Y. Chen, M. Yuan, H. Wang, R. Yu, and L. Hua, "Progressive optimization on structural design and weight reduction of CFRP Key Components", *International Journal of Lightweight Materials and Manufacture*, vol. 6, no. 1, pp. 59–71, 2023, doi: 10.1016/j.ijlmm.2022.07.001.

[20] M.A. Dybizbański and K. Rzeszut, "Badania laboratoryjne wzmacnianych belek stalowych cienkościennych typu sigma za pomocą tkanin CFRP z zastosowaniem bezdotykowych metod optycznych", *Przegląd Budowlany*, vol. 94, no. 7–8, pp. 111–116, 2023, doi: 10.5604/01.3001.0053.8501.

[21] K. Rzeszut and M.A. Dybizbański, "Structural behavior of sigma-type thin-walled cold-formed steel beams reinforced with CFRP textile", *ce/papers*, vol. 6, no. 3–4, pp. 11–15, 2023, doi: 10.1002/cepa.2747.

[22] J. Jönsson, "Distortional theory of thin-walled beams", *Thin-Walled Structures*, vol. 33, no. 4, pp. 269–303, 1999, doi: 10.1016/S0263-8231(98)00050-0.

Badania eksperymentalne na stalowych cienkościennych belkach typu sigma wzmocnionych tkaninami CFRP

Słowa kluczowe: belki cienkościenne, połączenie klejone, przekrój otwarto-zamknięty, stal zimnogięta, tkanina CFRP

Streszczenie:

Badanie miało na celu sprawdzenie, czy tkanina CFRP może być używana do zamknięcia profilu cienkościennej belki stalowej typu sigma w wybranych obszarach. Testy przeprowadzono na 16 próbkach, obejmując belki referencyjne (niewzmocnione) i trzy różne rozwiązania wzmocnienia, a także dwa różne przekroje poprzeczne. Testy obejmowały dwa etapy, z użyciem podpór widełkowych na obu końcach belki. W etapie II zablokowano dodatkowo możliwość deplanacji przekroju poprzecznego. Testy laboratoryjne wykorzystywały między innymi system ARAMIS i skaner 3D Artec Leo. Analizowano porównawczo przemieszczenia pionowe i poziome oraz opracowano wykresy siły-przemieszczenia globalne i lokalne. Metoda wzmocnienia może istotnie zwiększyć nośność cienkościennej belki stalowej o przekroju poprzecznym w postaci litery Sigma, które mają tendencję do deformacji w postaci otwarcia przekroju. Belki poddano testom w układzie czteropunktowego zginania. Tkanina CFRP (Sika Wrap 230C) była przyklejana do belki klejem SikaDur 330. Testy przeprowadzono przy użyciu maszyny wytrzymałościowej INSTRON 8505. Pomiary przemieszczeń były synchronizowane z przyrostem obciążenia z maszyny wytrzymałościowej i prezentowane w postaci filmów i wykresów za pomocą systemu pomiarowego ARAMIS. Propozycja wzmocnienia belki cienkościennej stali za pomocą tkanin CFRP może istotnie zwiększyć jej nośność. Szczególnie dla belki o smukłym przekroju, która ma tendencję do deformacji w postaci otwarcia przekroju. Metoda ta jest łatwa w aplikacji i ma minimalny wpływ na zwiększenie masy konstrukcyjnej elementu. Dodatkowe badania są jednak potrzebne w celu opracowania precyzyjnych wytycznych dotyczących zastosowania tej metody.

Received: 2024-03-25, Revised: 2024-05-21